Progress in Natural Science: Materials International 26 (2016) 283–288

HOSTED BY

ELSEVIER

Contents lists available at ScienceDirect

Progress in Natural Science: Materials International

journal homepage: www.elsevier.com/locate/pnsmi

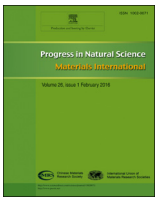

Original Research

Double carbon decorated lithium titanate as anode material with high rate performance for lithium-ion batteries

Haifang Ni, Weili Song, Lizhen Fan *

Institute of Advanced Materials and Technology, University of Science and Technology Beijing, Beijing 100083 China

ARTICLE INFO

Article history:
Received 30 March 2016
Accepted 20 April 2016
Available online 30 May 2016

Keywords:
Lithium titanate
Carbon nanotubes
Lithium-ion batteries
Anode materials

ABSTRACT

Spinel lithium titanate ($Li_4Ti_5O_{12}$) has the advantages of structural stability, however it suffers the disadvantages of low lithium-ion diffusion coefficient as well as low conductivity. In order to solve issues, we reported a simple method to prepare carbon-coated $Li_4Ti_5O_{12}$/CNTs (C@$Li_4Ti_5O_{12}$/CNTs) using stearic acid as surfactant and carbon source to prepare carbon coated nanosized particles. The obtained $Li_4Ti_5O_{12}$ particles of 100 nm in size are coated with the carbon layers pyrolyzed from stearic acid and dispersed in CNTs matrix homogeneously. These results show that the synthesized C@$Li_4Ti_5O_{12}$/CNTs material used as anode materials for lithium ion batteries, presenting a better high-rate performance (147 mA h g^{-1} at 20 C). The key factors affecting the high-rate properties of the C@$Li_4Ti_5O_{12}$/CNTs composite may be related to the synergistic effects of the CNTs matrix and the carbon- coating layers with conductivity enhancement. Additionally, the amorphous carbon coating is an effective route to ameliorate the rate capability of $Li_4Ti_5O_{12}$/CNTs.

1. Introduction

Due to its high energy density and long cycle life, rechargeable lithium ion batteries (LIBs) have attracted more attention in the past few decades and widely used in automobiles, electric vehicles and energy storage [1–3]. Taking into account the safety, cost and environmental concerns, graphite as the current commercial lithium ions anode material can not satisfy the requirements of practical applications [4]. Among the candidates, spinel lithium titanate ($Li_4Ti_5O_{12}$) has received the widespread attention in recent years for high power LIBs material due to its intrinsic properties, such as structural stability, high security, environment friendly, and low cost [5–7]. In addition, $Li_4Ti_5O_{12}$ has a wide charge/discharge platform of about 1.55 V (vs. Li/Li^+), which avoids the formation of solid electrolyte interface film and inhibits the deposition of lithium dendrite [8–11]. However, it suffers from some kinetic problems with poor electrical conductivity and low lithium diffusion coefficient, which results in the great decrease of charge/discharge capability. To overcome the above problems of $Li_4Ti_5O_{12}$, many strategies have been reported to enhance the electrochemical characteristics of $Li_4Ti_5O_{12}$ materials, including decreasing the particles size and designing the hierarchically structure of $Li_4Ti_5O_{12}$ [12–15], incorporating the second phase with high electronic conductivity such as carbon material modification or metal particles [16–20], and doping with other metal/ nonmetal ions [21–26].

In all these efforts, pyrolytic carbon-coated along with nanotechnology is considered to be a more effective method to improve the high rate discharge performance owing to the enhancement in the conductivity as well as the shortened the diffusion of lithium ions and electrons. Generally speaking, the introduced carbon-coated in the $Li_4Ti_5O_{12}$/C materials is amorphous in structure, making it hard to ameliorate the high-rate discharge property of the $Li_4Ti_5O_{12}$ anode material. Carbon nanotube (CNTs) possess a one-dimensional tubular structure with an aspect ratio up to 1000, has considered to be an excellent matrix to composite materials due to its inherent characteristics, such as high electrical conductivity, large surface area, chemical and mechanical stability [27–30]. In our previous work, it was found that the addition of carbon nanotubes as matrix can effectively enhance the rate property of $Li_4Ti_5O_{12}$ [28]. For $Li_4Ti_5O_{12}$/CNTs, due to the nanoparticles only some contact with carbon nanotubes, its high-rate discharge performance is greatly limited by the low surface electronic conductivity. Pyrolytic carbon coating technology has been approved to be an effective method to ameliorate the rate property of $Li_4Ti_5O_{12}$ anode material.

In this paper, the electrochemical performance of $Li_4Ti_5O_{12}$/CNTs electrode is greatly improved by coating with a thin amorphous carbon layer on the $Li_4Ti_5O_{12}$ nanoparticles/CNTs hybrid using a simple liquid phase deposition technique and subsequent calcination. Owing to the low thermal decomposition

* Corresponding author.
E-mail address: fanlizhen@ustb.edu.cn (L. Fan).
Peer review under responsibility of Chinese Materials Research Society.

http://dx.doi.org/10.1016/j.pnsc.2016.05.005

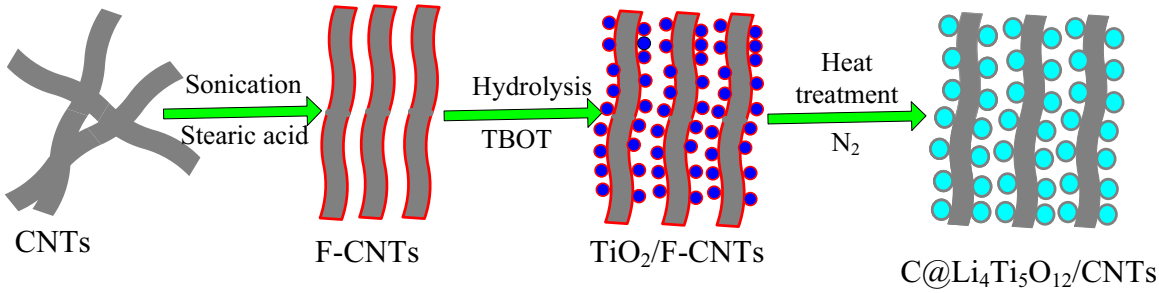

Fig. 1. Schematic illustration of the synthesis of C@$Li_4Ti_5O_{12}$/CNTs.

temperature and long-chain structure, stearic acid (SA) is used as an ideal organic carbon sources to form a thin amorphous carbon layer for coating $Li_4Ti_5O_{12}$ particle surface. In these hybrid electrodes, $Li_4Ti_5O_{12}$ nanoparticles are well wrapped between CNTs and the thin carbon layer. The combination of CNTs and carbon layer contributes to create a 3-dimensional (3D) conductive network to provide cross channel for electrolyte absorption and overcome the agglomeration and growth of $Li_4Ti_5O_{12}$ nanoparticles. In addition, the $Li_4Ti_5O_{12}$ nanoparticles surface coated with carbon layer can effectively separate CNTs and further set up cross conducting network to inhibit nanoparticle growth. As a result, the target product C@$Li_4Ti_5O_{12}$/CNTs show synergistic effect and display superior high rate performance and outstanding cycling stability as the anode materials for LIBs.

2. Experimental

The CNTs was purchased from Shenzhen Nanotech Port Co. Ltd. All other reactants were analytically pure and used without further purification.

The C@$Li_4Ti_5O_{12}$/CNTs were synthesized by an in situ liquid phase deposition route. The amount of CNT in C@ $Li_4Ti_5O_{12}$/CNTs was predetermined by 10 wt%. The predetermined amounts of stearic acid in C@$Li_4Ti_5O_{12}$/CNTs were 6, 12 and 24 wt%, respectively. Take 6 wt% stearic acid for example, 0.06 g stearic acid and 0.1 g CNTs were ultrasonically dispersed in 50 mL ethanol for 1 h, followed by the addition of tetrabutyl titanate solution (3.4 g) to form a suspension. Then, 0.562 g lithium acetate was dissolved into 1 mL water and 29 mL ethanol, and then dropped into the above suspension slowly. Continue to stir after 24 h, the mixed solution was treated at 60 °C in drying oven. The precursor was calcined at 400 °C for 4 h, and heated up to 750 °C for another 10 h under N_2 to obtain C@$Li_4Ti_5O_{12}$/CNTs. In contrast, $Li_4Ti_5O_{12}$/CNTs were also prepared under the same condition without the presence of stearic acid.

The morphologies and microstructures analyses of the as-synthesized powders were conducted by Rigaku/mac250 X-ray diffraction (XRD), ZEISS supra 55 field emission scanning electron microscopy (FE-SEM) and JEOL JEM-200CX transmission electron microscopy (TEM). The carbon contents in C@$Li_4Ti_5O_{12}$/CNTs were determined by an EMIA-820V carbon-sulfur analyzer. Electrochemical performances of $Li_4Ti_5O_{12}$/CNTs and C@$Li_4Ti_5O_{12}$/CNTs were investigated in CR2032 coin-type cells. The working electrodes were composed of active material, carbon black and polyvinylidene fluoride (8:1:1 in weight) on Cu foil. Battery assembled were conducted in an argon-filled glove box using a metallic lithium foil as the counter electrode, a Celgard 2400 polypropylene film as the separator and 1 M $LiPF_6$ in ethylene carbonate, dimethyl carbonate and ethylmethyl carbonate (1:1:1 in volume) as the electrolyte. The charge/discharge properties were tested on LAND CT2001A battery test system (Wuhan Jinnuo Electronics, Ltd.) at room temperature. Tested voltage window and current densities were 1.0–2.5 V and 0.2–20 C, respectively. The electrochemical impedance spectra (EIS) were measured at room temperature on a CHI660C electrochemical workstation (Shanghai Chenhua Co.). The amplitude of the AC signal was 5 mV over a frequency range of 100 kHz–0.01 Hz.

3. Results and discussion

Based on the above, our synthetic route was different from the previous reported synthesis of carbon-coated $Li_4Ti_5O_{12}$/CNTs materials, in which the $Li_4Ti_5O_{12}$ nanoparticles and CNTs were mixed mechanically for each other [31–33]. The overall fabrication procedure of the C@ $Li_4Ti_5O_{12}$/CNTs is schematically illustrated in Fig. 1. Firstly, CNT surface was functionalized using stearic acid, which facilitates the dispersion of CNTs in the ultrasound treatment. Then, TiO_2 nanoparticles were uniformly coated on the CNTs surface by controlled hydrolysis of tetrabutyl titanate. Finally, the TiO_2/CNTs were in situ transformed into $Li_4Ti_5O_{12}$/CNTs and the carbon layers coated on $Li_4Ti_5O_{12}$ nanoparticles surface were achieved by annealing for pyrolysis of stearic acid.

Fig. 2 shows the XRD patterns of the C@$Li_4Ti_5O_{12}$/CNTs with different stearic acid contents. It is observed that the majority of the diffraction peaks of all the samples can be identified as the spinel structure $Li_4Ti_5O_{12}$ (JCPDS Card No.49-0207). It is obvious that no diffraction peaks appear for CNTs matrix and carbon from pyrolysis of stearic acid due to its amorphous structure. In other word, the presence of the carbon does not influence the structure of $Li_4Ti_5O_{12}$. In addition, with the increase of the amount of stearic acid, the intensity of the diffraction peak of the C@$Li_4Ti_5O_{12}$/CNTs is significantly increased. It is very obvious that minor impurity

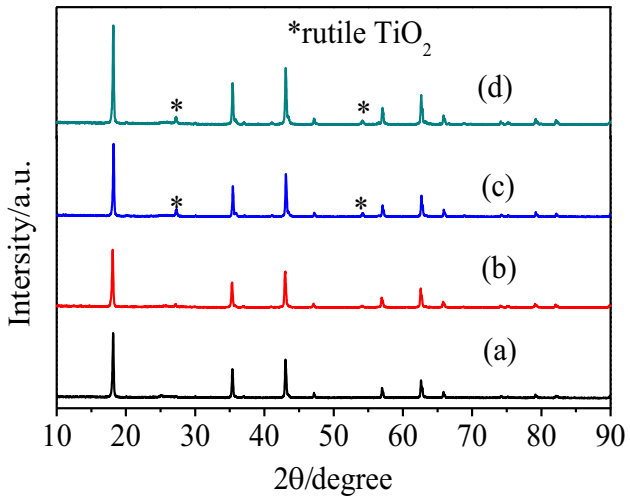

Fig. 2. XRD patterns of (a) $Li_4Ti_5O_{12}$/CNTs, (b) C@$Li_4Ti_5O_{12}$/CNTs with 6 wt% stearic acid, (c) C@$Li_4Ti_5O_{12}$/CNTs with 12 wt% stearic acid and (d) C@$Li_4Ti_5O_{12}$/CNTs with 24 wt% stearic acid.

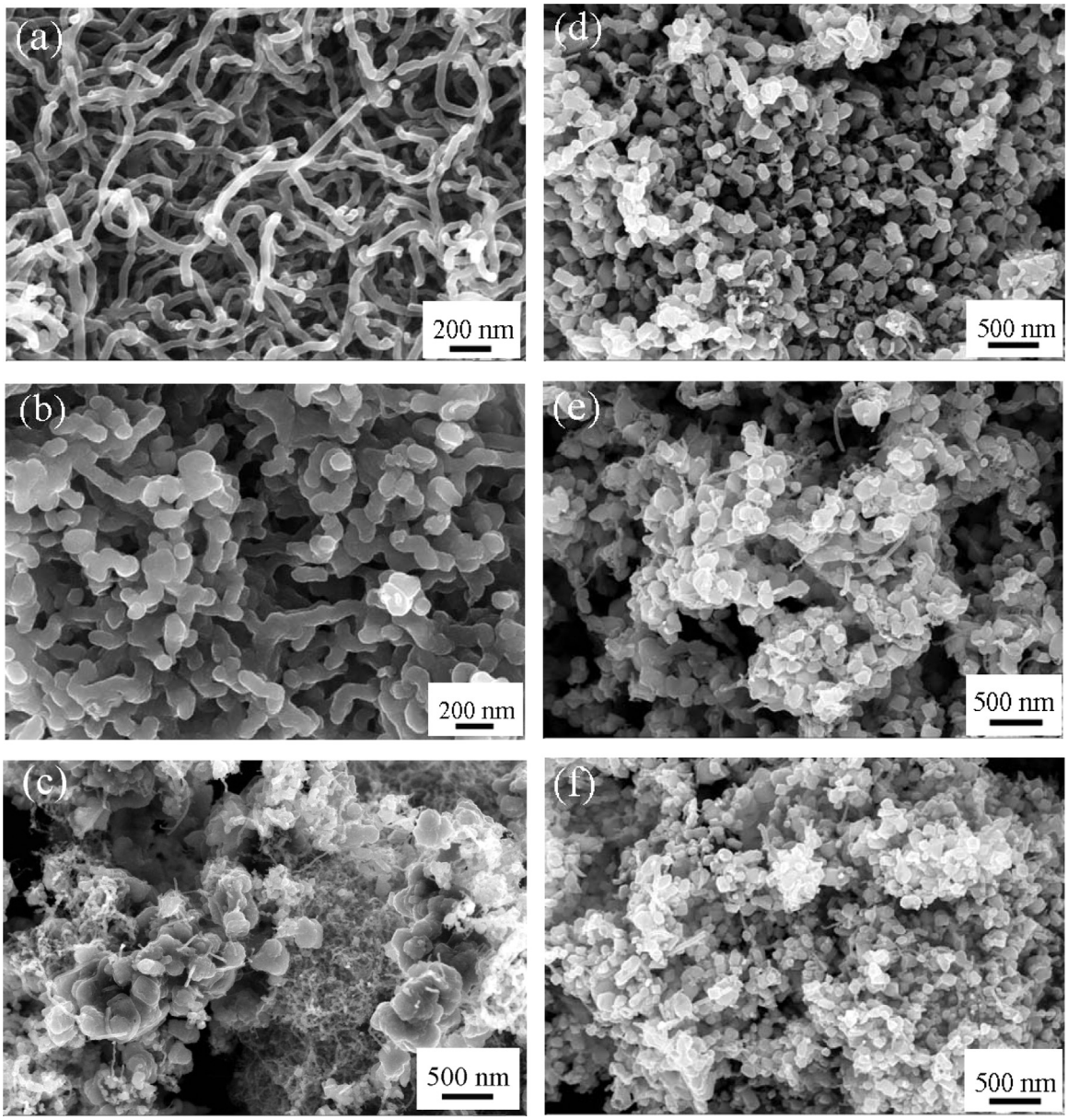

Fig. 3. SEM images of (a) CNTs, (b)TiO_2/CNTs, (c) $Li_4Ti_5O_{12}$/CNTs, (d) C@$Li_4Ti_5O_{12}$/CNTs with 6 wt% stearic acid, (e) C@$Li_4Ti_5O_{12}$/CNTs with 12 wt% stearic acid and (f) C@$Li_4Ti_5O_{12}$/CNTs with 24 wt% stearic acid.

was detected for C@$Li_4Ti_5O_{12}$/CNTs (12 wt% and 24 wt% stearic acid), which can be identified as rutile TiO_2. This minor impurity could have been induced because of the shortage of lithium source, which evaporates due to the higher-temperature treatments. Based on results of carbon-sulfur analysis, the carbon content (CNTs + pyrolysis carbon) in the C@$Li_4Ti_5O_{12}$/CNTs with 0, 6, 12 and 24 wt% of stearic acid is about 9.6, 9.9, 10.1 and 10.4 wt%, respectively.

Fig. 3 shows the FESEM images of CNTs, TiO_2/CNTs, and C@$Li_4Ti_5O_{12}$/CNTs coated with different carbon contents. The representative SEM image (Fig. 3a) reveals that the randomly entangled multi-walled CNTs have an outer diameter of approximately 50 nm, and the interconnected carbon tubes form a 3D network structure. The TiO_2 coated on the CNTs was obtained by the control hydrolysis of tetrabutyl titanate in the CNTs matrix (Fig. 3b), which can clearly see that individual CNTs surface evenly covered a layer of TiO_2 film. After these two-step annealing procedures, the 1D structure TiO_2/CNTs were in situ transformed into $Li_4Ti_5O_{12}$/CNTs, which are beneficial to homogenous dispersion of nanoparticles into CNTs matrix, and in turn prevents the intertwining of CNTs during thermal reduction process (Fig. 3d). It is noted that the material prepared in the absence of stearic acid consisted of intertwine CNTs and irregular aggregates with the size of 300–800 nm (Fig. 3c). With increasing amount of stearic acid in the precursors, some particles attached together due to increased carbon content (Fig. 3e and f).

In order to understand the microstructures and crystal structures, TEM and HRTEM analysis of the C@$Li_4Ti_5O_{12}$/CNTs with 6 wt% stearic acid was also conducted. The TEM image displays $Li_4Ti_5O_{12}$ nanoparticles with a size of $\sim$100 nm are dispersed in CNTs matrix and some of the smaller particles ($<$ 50 nm) are also attached on the carbon wall (Fig. 4a). According to the HRTEM image, the disordered phase coated on the $Li_4Ti_5O_{12}$ surface is the carbon-layer derived from stearic acid decomposition, and the carbon layer connects with the $Li_4Ti_5O_{12}$ particles and outer CNTs, which confirmed the formation of the C@ $Li_4Ti_5O_{12}$/CNT hybrid conductive network. The thickness of the carbon layer connected the $Li_4Ti_5O_{12}$ particles and outer CNTs is about 2 nm, which is

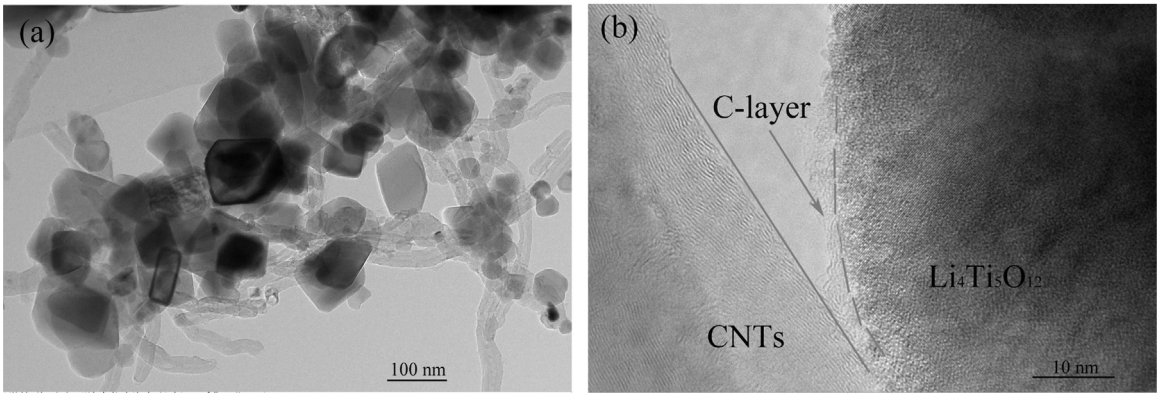

Fig. 4. TEM image (a) and high resolution TEM image (b) of C@$Li_4Ti_5O_{12}$/CNTs with 6 wt% stearic acid.

beneficial to the lithium ion transport between $Li_4Ti_5O_{12}$ particles and the electrolyte (Fig. 4b). Furthermore, the presence of this carbon layer coated on the $Li_4Ti_5O_{12}$ particles surface is conducive to limit the particle growth of $Li_4Ti_5O_{12}$ and ameliorate the electrical conductivity of the materials, thus improving the high-rate performance.

Fig. 5 gives the first charge/discharge curves of the C@$Li_4Ti_5O_{12}$/CNTs and $Li_4Ti_5O_{12}$/CNTs in the potential ranges of 1.0–2.5 V at a rate of 0.2 C and 10 C. It is very obvious that all the

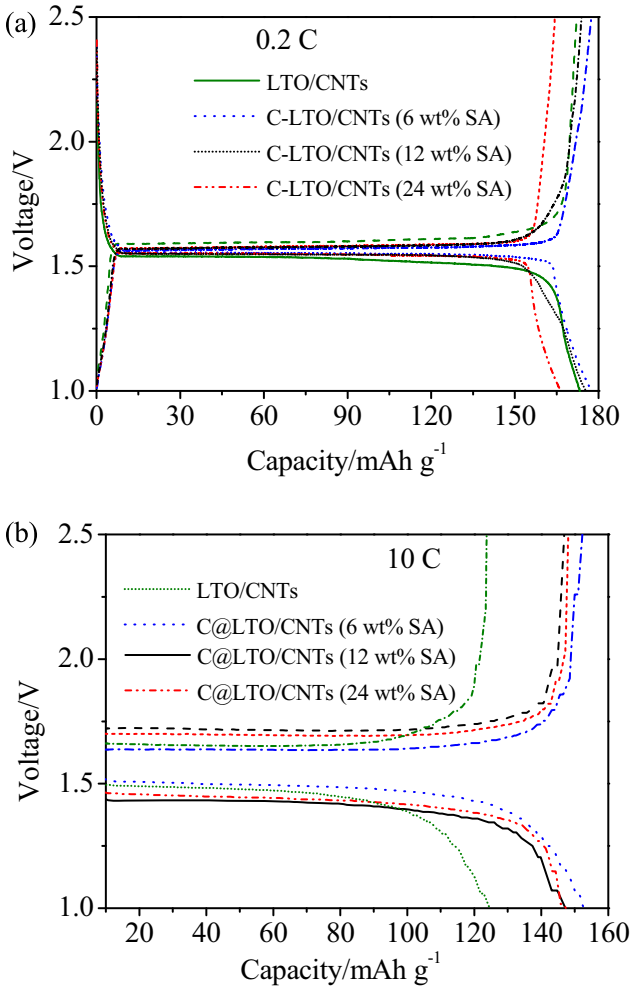

Fig. 5. Galvanostatic charge/discharge curves of $Li_4Ti_5O_{12}$/CNTs, C@$Li_4Ti_5O_{12}$/CNTs (6 wt% stearic acid), C@$Li_4Ti_5O_{12}$/CNTs (12 wt% stearic acid), C@$Li_4Ti_5O_{12}$/CNTs (24 wt% stearic acid) at (a) 0.2 C and (b) 10 C.

electrodes display one charge plateaus and corresponding discharges plateaus, which is corresponding to the two-phase electrochemical reactions. These results suggest that the present of carbon does not influence the redox reaction process. In comparison with the composites, the C@$Li_4Ti_5O_{12}$/CNTs coated with 0.3 wt% carbon has longer and narrower charge/discharge plateaus, indicating that the as-prepared material has a relatively good electrical conductivity. As seen in Fig. 5, the first discharge capacities for C@ $Li_4Ti_5O_{12}$/CNTs at 0.2 C are 173.3 (0 wt% stearic acid), 177.4 (6 wt% stearic acid), 175.4 (12 wt% stearic acid) and 166.4 mA h g^{-1} (24 wt% stearic acid) (the capacity calculation only include the weight of $Li_4Ti_5O_{12}$). The first columbic efficiency of the C@ $Li_4Ti_5O_{12}$/CNTs with 0, 6, 12 and 24 wt% of stearic acid is 99.20, 99.88, 99.25 and 98.80 wt%, respectively. In all those samples, the highest the carbon content, the lowest reversible capacity is obtained. The main reason is that the reaction temperature during the heat treatment increase with in increasing the amounts of stearic acid, which leads to the existence of mixed phase (rutile TiO_2) in the final product. The existence of this impurity would damage to the charger/discharge properties due to the conductivity of the rutile TiO_2 is lower than that of $Li_4Ti_5O_{12}$ [22–25]. Furthermore, excessive carbon content could also limit the diffusion of lithium ions. Remarkably, with increasing current density (10 C), the voltage plateau becomes shorter and the charge voltage plateau rises with drop of discharge voltage plateau due to the increasing polarization. The C@$Li_4Ti_5O_{12}$/CNT electrode (6 wt% stearic acid) delivers more reversible specific capacity, which can be attributed to the improvement of electrical conductivity and the decreasing of particle size in the $Li_4Ti_5O_{12}$ (Fig. 4b).

To examine the effectiveness of carbon-coated layer in affecting the rate performance of the electrodes, the rate capabilities of C@$Li_4Ti_5O_{12}$/CNTs and $Li_4Ti_5O_{12}$/CNTs electrodes are investigated in Fig. 6. It is found that the capacity values drop with increasing the current density, which is associated with the limited Li-ion diffusion kinetics at very high current density. However, for the $Li_4Ti_5O_{12}$/CNTs electrode, the larger size of particle leads to prolonging the lithium ion diffusion from surface to central part, the discharge capacity decreases sharply with an increasing discharge rate. However, at the same rate, the capacity of the C@$Li_4Ti_5O_{12}$/CNTs electrodes decrease much slower due to the well crystallized and fined particle size, ensuring a better electrochemical performance. It is obvious that the capacity obtained by C@$Li_4Ti_5O_{12}$/CNTs (6 wt% stearic acid) at current density of 20 C is higher than that obtained at current density of 5 C for $Li_4Ti_5O_{12}$/CNTs. The rate capability of the C@$Li_4Ti_5O_{12}$/CNTs electrodes is improved significantly. It should be noted that the specific capacity of the C@$Li_4Ti_5O_{12}$/CNTs (6 wt% stearic acid) is 147.2 mA h g^{-1} at the rate of 20 C, which is higher than that obtained at the same rate for the $Li_4Ti_5O_{12}$/CNTs in our previous work

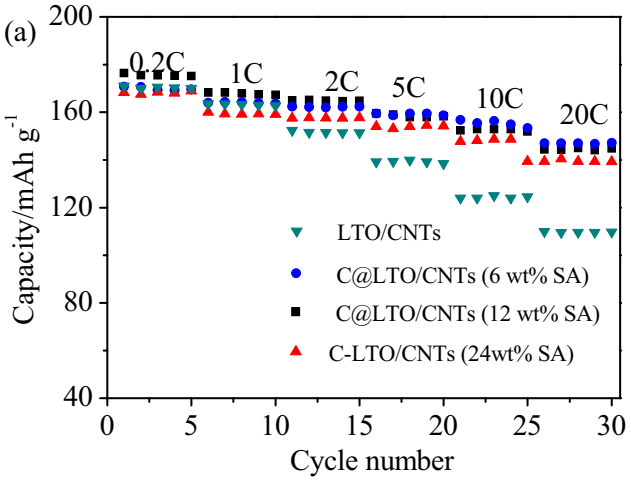

Fig. 6. Comparison of rate capability of $Li_4Ti_5O_{12}$/CNTs, C@$Li_4Ti_5O_{12}$/CNTs (6 wt% stearic acid), C@$Li_4Ti_5O_{12}$/CNTs (12 wt% stearic acid) and C@$Li_4Ti_5O_{12}$/CNTs (24 wt% stearic acid).

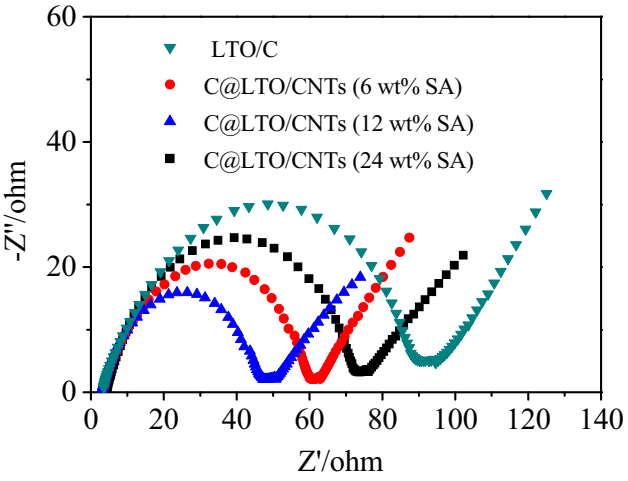

Fig. 8. EIS curves of $Li_4Ti_5O_{12}$/CNTs, C@$Li_4Ti_5O_{12}$/CNTs (6 wt% stearic acid), C@$Li_4Ti_5O_{12}$/CNTs (12 wt% stearic acid) and C@$Li_4Ti_5O_{12}$/CNTs (24 wt% stearic acid) electrodes at the voltage of 1.56 V.

(112 mA h g^{-1}). It is suggested that the excellent rate capability of the C@ $Li_4Ti_5O_{12}$/CNTs electrodes is related to their good crystallinity and high surface electrical conductivity.

Fig. 7 shows the cycling performance of $Li_4Ti_5O_{12}$/CNTs and

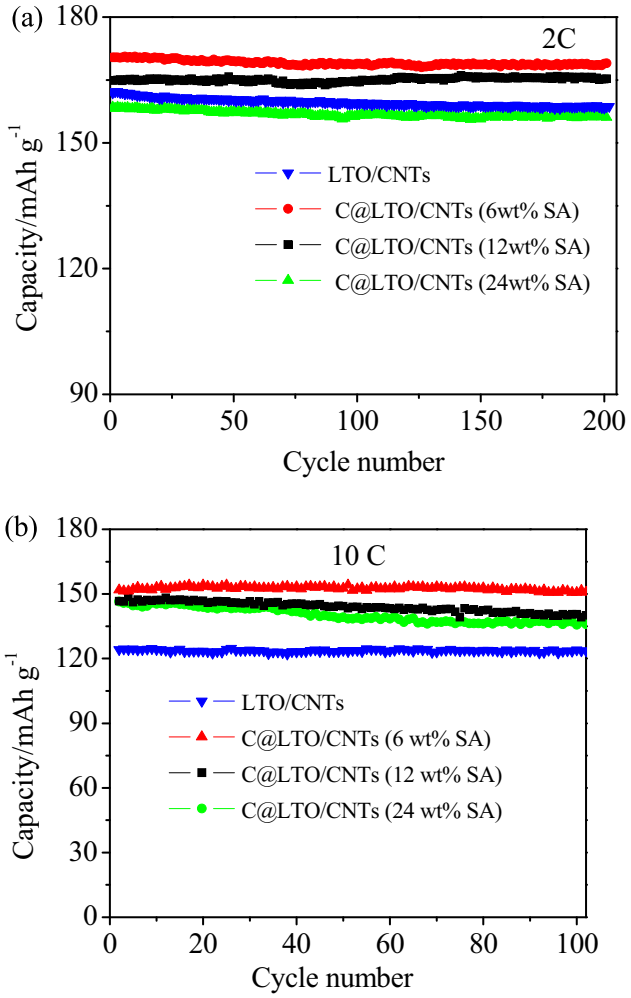

Fig. 7. Cycle performance of $Li_4Ti_5O_{12}$/CNTs, C@$Li_4Ti_5O_{12}$/CNTs (6 wt% stearic acid), C@$Li_4Ti_5O_{12}$/CNTs (12 wt% stearic acid) and C@$Li_4Ti_5O_{12}$/CNTs (24 wt% stearic acid) at (a) 2 C and (b)10 C.

C@$Li_4Ti_5O_{12}$/CNTs at 2 C and 10 C in the potential ranges of 1.0–2.5 V. Obvious, the capacities of all the electrodes are dropped considerably over 100 cycles (Fig. 7). In other words, all the electrodes display excellent cycle stability, which can be ascribed to the improvement of the electronic conductivity by the CNTs substrate and in situ carbon coated layer and the intrinsic structure stability of $Li_4Ti_5O_{12}$.

In order to understand the introducing of carbon-coated layer on the high-rate property of C@$Li_4Ti_5O_{12}$/CNTs, the electrochemical impedance spectrum of the all products were further investigated. Fig. 8 gives the impedance spectrum of C@$Li_4Ti_5O_{12}$/CNTs at discharge state. It is clearly seen that each of the spectra include high-frequency semicircle and low-frequency oblique line, which are correspond to the charge-transfer process and lithium ions diffusion, respectively. It is obvious that the C@$Li_4Ti_5O_{12}$/CNTs electrodes show lower charge-transfer resistance than $Li_4Ti_5O_{12}$/CNTs electrode, suggesting that their electrochemical reaction between electrode and electrolyte occur easily. Since the redox reaction is determined by electronic conduction and ion transport, the decrease of impedance means the improvement of the electrical conductivity of the C@$Li_4Ti_5O_{12}$/CNTs electrodes. This is caused by the co-modification of pyrolytic carbon layer and CNTs substrate. It is quite apparent that the C@$Li_4Ti_5O_{12}$/CNTs (12 wt% stearic acid) electrode shows the lowest charge-transfer resistance. This result may be due to the appropriate amount of carbon-coated content. The improvement of the high-rate properties of the C@$Li_4Ti_5O_{12}$/CNTs materials could be attributed to the synergistic effect of the hybrid structure. The $Li_4Ti_5O_{12}$ nanoparticles are uniformly dispersed in the interlaced CNTs, which act as the ideal substrate for fast lithium ions transport. The carbon layers are intimately attached on the CNTs and nanoparticles to form 3D conductive networks, which acts as a conductive matrix that is advantage to the electronic transmission. It is generally accepted that such 3D hybrid structure consist of 0D nanoparticles, 1D CNTs, and 2D carbon-coated layers will be widely used in electrochemical energy materials and other fields.

4. Conclusions

In summary, C@$Li_4Ti_5O_{12}$/CNTs composites have been fabricated by liquid deposition, in which the TiO_2 was first deposited on the CNTs substrate and then in situ transformed into $Li_4Ti_5O_{12}$. In this way, the $Li_4Ti_5O_{12}$ particles are intimately embedded and

exclusively confined in an interconnected CNTs matrix with high electrical conductivity. In additions, the carbon layer coating on the surface of $Li_4Ti_5O_{12}$ particles which derived from the decomposition of stearic acid can also further improve the electrical conductivity. By combining such unique features, the prepared C@$Li_4Ti_5O_{12}$/CNTs composite present excellent high-rate discharge ability and cycling stability.

Acknowledgements

Financial supports from 973 Project (2015CB932500), NSF of China (51532002, 51372022, 51575030 and 51302011) are gratefully acknowledged.

References

[1] M.S. Wang, L.Z. Fan, M. Huang, et al., J. Power Sources 219 (2012) 29–35.
[2] Y. Guo, J. Hu, L. Wan, Adv. Mater. 20 (15) (2008) 2878–2887.
[3] H.C. Tao, L.Z. Fan, W.L. Song, Nanoscale 6 (6) (2014) 3138–3142.
[4] S. Zhang, K. Xu, T. Jow, J. Power Sources 160 (2) (2006) 1349–1354.
[5] L. Shen, B. Ding, P. Nie, et al., Adv. Energy Mater. 3 (11) (2013) 1484–1489.
[6] H.F. Ni, W.L. Song, L.Z. Fan, Electrochem. Commun. 40 (2014) 1–4.
[7] L. Shen, E. Uchaker, X. Zhang, et al., Adv. Mater. 24 (48) (2012) 6502–6506.
[8] H. Xia, W. Sun, L. Peng, et al., Chem. Commun. 51 (72) (2015) 13787–13790.
[9] H.F. Ni, L.Z. Fan, J. Chin, Ceram. Soc. 40 (4) (2012) 548–554.
[10] G. Cao, L. Shen, H. Li, et al., Nano Lett. 12 (2012) 5673–5678.
[11] C. Ouyang, Z. Zhong, M. Lei, Electrochem. Commun. 9 (5) (2007) 1107–1112.
[12] J. Liao, V. Chabot, M. Gu, Nano Energy 9 (2014) 383–391.
[13] K. Kim, C. Yu, C. Yoon, Nano Energy 12 (2015) 725–734.
[14] Y. Sha, B. Zhao, R. Ran, J. Mater. Chem. A 1 (42) (2013) 13233–13243.
[15] J. Cheng, R. Che, C. Liang, et al., Nano Res. 7 (7) (2014) 1043–1053.
[16] M. Li, D. Zhou, W.L. Song, L.Z. Fan, J. Mater. Chem. A 3 (2015) 19907–19912.
[17] M.S. Wang, W.L. Song, L.Z. Fan, Chem. Electro. Chem. 2 (2015) 1699–1706.
[18] D. Zhou, W.L. Song, L.Z. Fan, ACS Appl. Mater. Inter 7 (38) (2015) 21472–21478.
[19] M.S. Wang, W.L. Song, L.Z. Fan, J. Mater. Chem. A 3 (24) (2015) 12709–12717.
[20] T.T. Liu, H.F. Ni, W.L. Song, L.Z. Fan, J. Alloy. Compd. 646 (2015) 189–194.
[21] C. Chen, Y. Huang, C. An, et al., Chem. Sus. Chem. 8 (1) (2015) 114–122.
[22] N. Li, G. Zhou, F. Li, et al., Adv. Funct. Mater. 23 (43) (2013) 5429–5435.
[23] L. Shen, E. Uchaker, X. Zhang, et al., Adv. Mater. 24 (48) (2012) 6502–6506.
[24] M. Ji, Y. Xu, Z. Zhao, et al., J. Power Sources 263 (2014) 296–303.
[25] H.F. Ni, W.L. Song, L.Z. Fan, Ionics 21 (12) (2015) 3169–3176.
[26] Q. Zhang, H. Lu, H. Zhong, J. Mater. Chem. A 3 (2015) 13706–13716.
[27] Z. Yu, L. Tetard, L. Zhai, et al., Energy Environ. Sci. 8 (3) (2015) 702–730.
[28] H.F. Ni, L.Z. Fan, J. Power Sources 214 (2012) 195–199.
[29] A. Reddy, S. Gowda, M. Shaijumon, Adv. Mater. 24 (37) (2012) 5045–5064.
[30] J. Zhang, Y. Hu, J. Tessonnier, Adv. Mater. 20 (8) (2008) 1450–1455.
[31] X. Li, P. Huang, Y. Zhou, et al., Mater. Lett. 133 (2014) 289–292.
[32] J. Wang, W. Li, Z. Yang, et al., RSC Adv. 4 (48) (2014) 25220–25226.
[33] L. Wang, H. Zhang, Q. Deng, Electrochim. Acta 142 (2014) 202–207.